An Experimental Method for the Percutaneous Induction of a Posterolateral Infarct and Functional Ischemic Mitral Regurgitation

Thomas M. Joudinaud, Corrine L. Kegel, Alan A. Gabster, Mark L. Sanz, Alistair MacDonald, Dan Propp, Edward Callaghan, Patricia A. Weber, Ulrik Hvass[1], Carlos M. G. Duran

The International Heart Institute of Montana Foundation at Saint Patrick Hospital and Health Sciences Center and The University of Montana, Missoula, Montana, USA, [1]Hôpital Bichat, Service de Chirurgie Cardiaque, Paris, France

Background and aim of the study: **Appropriate experimental models are needed to study the mechanisms underlying left ventricular (LV) remodeling and functional ischemic mitral regurgitation (IMR). Herein is described an original percutaneous method for inducing a well-defined posterolateral infarct and significant IMR.**

Methods: **Under videofluoroscopic guidance, the second (OM2) and third (OM3) obtuse marginal branches of the circumflex artery of six sheep were selectively and sequentially injected with 100% ethyl alcohol. Transthoracic echocardiography (TTE) was performed before and after alcohol injection, and weekly until sacrifice at 8 ± 1.3 weeks. The LV end-systolic (LVESD) and end-diastolic (LVEDD) dimensions, interpapillary distance (M1-M2), mitral annulus diameter (MA), and degree of IMR and ischemic tricuspid regurgitation (ITR) were measured.**

Results: **One animal died from irreversible ventricular fibrillation. In the remaining sheep, a well-defined posterolateral infarct of 22% of the heart mass resulted, followed by 2.8+ IMR and 2.1+ ITR. The mean weight gain was 16%, and all sheep showed signs of heart failure. All echocardiographic parameters were increased: systolic MA by 29%, diastolic MA by 18%, LVEDD by 33%, LVESD by 62%, M1-M2 diastolic by 32%, M1-M2 systolic by 21%, and tethering and tenting distances by 32% and 108%, respectively.**

Conclusion: **The percutaneous selective injection of 100% ethyl alcohol in OM2 and OM3 resulted in a well-defined posterolateral infarct and significant IMR and ITR. Because it was a percutaneous procedure, this novel, simple and reproducible method did not require a thoracotomy. This model should facilitate the further study of LV remodeling and IMR.**

The Journal of Heart Valve Disease 2005;14:460-466

Functional ischemic mitral regurgitation (IMR) is a serious complication of coronary artery disease, and carries a poor prognosis (1-3). In an attempt to advance our knowledge of the pathophysiology of this entity, numerous experimental studies have been conducted (4-6). The most popular chronic ovine model involves ligating branches of the circumflex artery to induce a posterolateral infarct, which results in significant IMR. This model, although highly reproducible and successful, requires a thoracotomy to occlude the target vessels (7). A subsequent reoperation is required to evaluate a particular surgical repair technique.

Presented as a poster at the Third Biennial Meeting of the Society for Heart Valve Disease, 17th – 20th June 2005, Vancouver Conference and Exhibition Centre, Vancouver, Canada

Address for correspondence:
Carlos M. G. Duran MD, PhD, The International Heart Institute of Montana Foundation, 554 West Broadway, Missoula, MT 59802, USA
e-mail: duran@saintpatrick.org

Alternatively, because of the high mortality associated with reoperation in sheep in heart failure, different surgical procedures are first performed prophylactically in healthy animals, followed by a second thoracotomy to occlude the coronary branches and induce a myocardial infarct.

A review of the alcohol treatment of hypertrophic cardiomyopathy (8-10) suggested a hypothesis for the possible induction of a posterolateral infarct using percutaneous selective injection of ethyl alcohol into the branches of the circumflex artery in an ovine model.

Materials and methods

Surgical procedure

Targhee sheep (bodyweight range 50-70 kg) were premedicated with intravenous (i.v.) ketamine (1.0 mg/kg), atropine (0.03 mg/kg) and propofol (4.0 mg/kg), and a left jugular catheter was placed in position. Artificial ventilation was maintained with a vol-

ume respirator (North American Drager, Telford, PA, USA) supplemented with oxygen at 4 l/min. Anesthesia was maintained with intermittent propofol and continuous isoflurane (1.5-2.5%). The sheep were heparinized with 10,000 U plus an additional 5,000 U/h infusion. A Swan-Ganz catheter was introduced through the left jugular vein into the pulmonary artery. At baseline, three consecutive sets of measurements of cardiac output, right ventricular (RV) pressure and pulmonary artery pressure (PAP) were taken.

A catheter (6 Fr Pinnacle; Terumo, Inc., Somerset, NJ, USA) was introduced via the left carotid by percutaneous puncture or cut down. An angiogram was performed using a c-arm (OEC 9400; GE Medical Systems, Inc., Waukesha, WI, USA) via a guiding catheter (LA6HS1, multipurpose hockey stick 1; Medtronic, Inc., Minneapolis, MN, USA) to identify the second (OM2) and third (OM3) obtuse marginal branches of the circumflex artery. A balloon catheter (D3S3020 Over-the-Wire Balloon Dilatation Catheter; Medtronic, Inc.) was positioned in the origin of OM2 and inflated beyond the first branch (4 bar). Therefore, the distal part of OM2 was isolated from the coronary circulation. Without deflating the balloon, 1-3 ml of 100% ethyl alcohol (EtOH) was injected into the distal part of OM2. After 5 min, the balloon was deflated and the heart allowed to recover for 30 min. The guidewire and the balloon catheter were then advanced into OM3, inflated again distal to its origin (4 bar), and 2-3 ml of 100% EtOH injected. It was decided empirically to limit the total volume of EtOH injected to 5 ml. After 5 min, the balloon catheter was deflated. Aortic pressure was recorded through the angiocatheter. Cardiac output and PAP were measured through the Swan-Ganz catheter before and after the procedure. During the entire procedure, amiodarone (40 mg/h) and lidocaine (4 mg/min) were infused to prevent arrhythmia. Before each EtOH injection, magnesium (1 g, i.v.), lidocaine (60 mg, i.v.) and bretylium (25 mg, i.v.) were injected into each animal.

Echocardiography

Transthoracic echocardiography (TTE) was performed before the procedure (baseline), after the procedure, at weekly intervals thereafter, and again at sacrifice. The sheep was positioned upright in a fenestrated sling for each TTE examination. The left ventricular end-systolic dimension (LVESD) and end-diastolic dimension (LVEDD) and the interpapillary muscle tips distance at end-systole (M1-M2s) and end-diastole (M1-M2d) were recorded through a short-axis view. The mitral valve annulus diameter was measured, and the presence of IMR and/or ischemic tricuspid regurgitation (ITR) evaluated in the long-axis view. The severity of IMR and of ITR was determined by the length of the jet (1+, present; 2+, half the distance to the atrial walls; 3+, reaching the atrial wall; 4+, for reverse pulmonary vein flow or if the jet reached the inferior vena cava) (11). Displacement of the papillary muscles was calculated as the distance between their tips and to the contralateral mitral annulus ('tethering distance'). Valve coaptation height or 'tenting distance' was measured as the distance between the leaflet's coaptation point and the mitral annulus plane at end-diastole. The ejection fraction was calculated using the Teichhotz formula for the end-diastolic and end-systolic volumes (12).

After 6-10 weeks, the animals were again anesthetized, and the chest was opened through the fourth intercostal space. An epicardial echocardiogram was performed to analyze LV function and the degree of IMR and ITR. A Swan-Ganz catheter was placed via the left jugular vein to record PAP, RV pressure and cardiac output. After heparinization with 10,000 U, the animal was euthanized with an injection of 60 mEq KCl in the ascending aorta, and the heart excised.

Cardiac histology

The hearts were cut into eight or nine 1 cm-thick transverse slices which were then incubated in 2% triphenyl tetrazolium chloride for 30 min at room temperature (13). The individual slices were weighed and photographed (Powershot A70; Canon USA, Inc., Lake Success, NY, USA). The RV and LV infarcted areas were quantified using planimetry software (AutoCAD; Autodesk, Inc., San Rafael, CA, USA) to delineate the LV from the RV tissue. The percentage of LV area infarcted was used to determine the LV mass infarcted. The slices were fixed in 10% formalin for histologic analysis. The fixed samples were dehydrated and embedded in PolyFin wax (Polyscience, Inc., Warrington, PA, USA), sectioned at 5 μm, and collected on Superfrost®-plus slides (VWR Scientific, West Chester, PA, USA). Representative sections were stained with hematoxylin and eosin for general tissue and cellular morphology.

Animal welfare

All animals were cared for in accordance with the *Principles of Laboratory Animal Care* formulated by the National Society of Medical Research and the *Guide for the Care and Use of Laboratory Animals* prepared by the Institute of Animal Resources, National Research Council, and published by the National Academy Press, revised 1996. The protocol for the use of the animals for this project was also reviewed and approved by the Institutional Animal Care and Use Committee (IACUC) of The University of Montana.

J Heart Valve Dis
Vol. 14. No. 4
July 2005

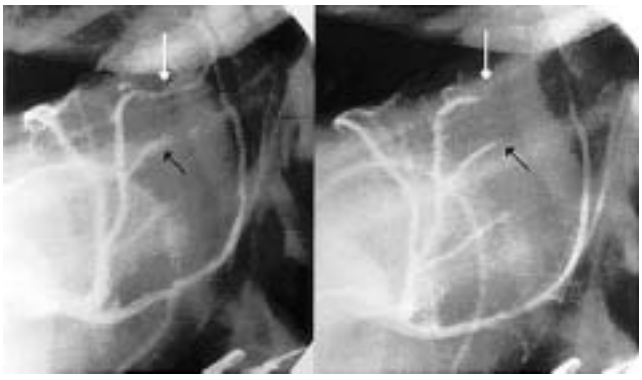

Figure 1: Coronary angiogram of the left coronary artery before (left) and after (right) the 100% ethanol injection in OM2 (black arrow) and OM3 (white arrow).

Statistical analysis

Data were evaluated with repeated measures analysis of variance (ANOVA) and explored by three paired Student's *t*-tests to compare each time point (baseline versus immediate post-infarction, post-infarction versus sacrifice, and baseline versus sacrifice). A p-value <0.016 was considered to be statistically significant (Bonferroni corrected).

Results

The EtOH ablation procedure was performed in six sheep with an average weight of 53.57 kg (range: 64.5 to 39.5 kg). The left carotid introducer was placed percutaneously in four sheep, and with a cut-down procedure in two. The baseline coronary angiograms showed that the LV apex was supplied by the left anterior descending artery in five sheep (type A), and by the circumflex branches in one sheep (type B). These findings were similar to those reported by Llaneras et al. (7). In five animals, it was easy to visualize OM1 and OM2 by videofluoroscopy. In four sheep, the coronary anatomy was similar. The origins of OM2 and OM3 were well-individualized branches off the circumflex artery. In three of these cases, each branch had two EtOH injections (Fig. 1). In one animal, OM2 and OM3 were very small, so the fourth marginal branch (OM4) was injected, followed by irreversible ventricular fibrillation that terminated the procedure. In two other cases (one type A and one type B), a large branch of the circumflex artery divided distally into OM2 and OM3. In these cases, a single bolus of EtOH was injected into the large branch (4 ml and 5 ml, respectively). The mean volume of EtOH injected was 1.5 ml in OM2 and 2.6 ml in OM3 (total of 4 ml/animal).

The hemodynamic and echocardiographic data at baseline and immediately after the procedure are listed in Table I. In all cases, frequent multiform ventricular non-sustained tachycardia occurred at the time of injection, which stopped spontaneously when the injection was terminated. In all animals, the electrocardiogram (ECG) showed severe ST segment elevation after the EtOH injection (Fig. 2).

Figure 2: S-T elevation segment of the electrocardiogram at the end of the procedure.

Five animals were followed for an average of 8 ± 1.3 weeks. The two animals with a single large OM that received only one injection of EtOH developed early clinical heart failure at two weeks post-procedure, requiring the administration of furosemide (20 mg twice weekly) followed by daily doses (20 mg) during the last week before sacrifice at six and seven weeks. The other three animals showed signs of clinical heart failure after the fourth week, and were sacrificed at eight and nine weeks.

At the time of sacrifice, all animals were in heart failure. They were breathing rapidly, had a pale nose, stretched their hind legs, increased their water intake, and retained fluid. The average weight increased by 16% (p = 0.043), from 56.4 ± 7.6 kg (range: 44.0 to 64.5 kg) to 65.3 ± 3.9 kg (range: 63.1 to 71.2 kg). The hemodynamic and ECG data at the end of the study are listed in Table I. The progressive echocardiographic changes during follow up are illustrated in Figure 3. At sacrifice, the mean grade of IMR was 2.8 ± 0.45+, and of ITR was 2.1 ± 0.5+. The LVEDD increased by 33.7 ±

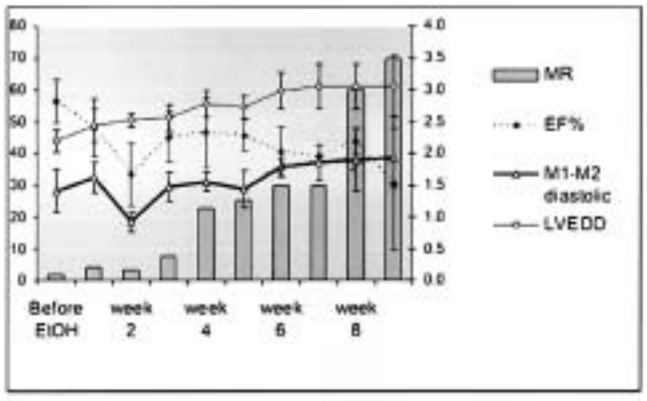

Figure 3: Time-related changes in degree of ischemic mitral regurgitation (MR), left ventricular ejection fraction (EF), left ventricular end diastolic dimension (LVEDD), and diastolic interpapillary muscle distance (M1-M2).

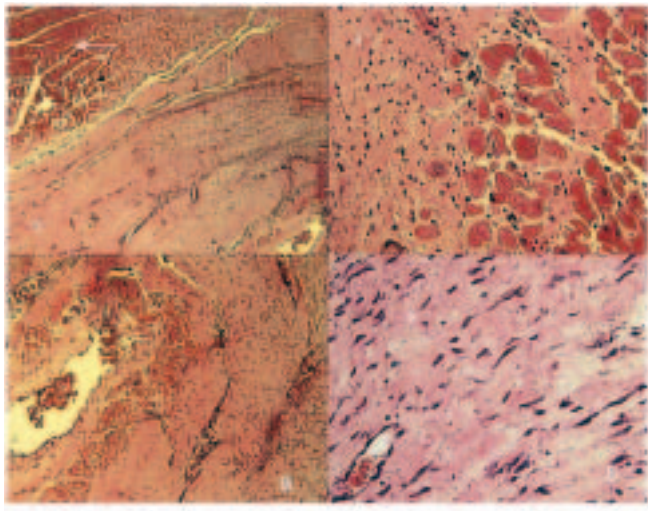

Figure 4: Histologic sections of the infarcted ventricular wall. A) Border zone showing living cardiomyocytes (upper left, white arrow) (original magnification, ×4). B) Small bundles of cardiac myocytes present in a subendocardial location (original magnification, ×10). C) Border zone showing bands of fibroblasts in a finely fibrillar background with bundles of cardiomyocytes (original magnification, ×40). D) Ghost cell (white arrow) collagen and fibroblast (original magnification, ×40).

17.0% (p = 0.009), and the LVESD by 62.0 ± 40.0% (p = 0.015), while the diastolic distance between the papillary muscles (M1-M2d) increased by 32.0 ± 24.0% (p = 0.01), and the systolic distance (M1-M2s) by 40.7 ± 32.0%. The tethering and tenting distances increased by 32.7 ± 28.0% and 108.0 ± 65.0% (p = 0.036), respectively. The mitral annulus diameter had enlarged by 18.46 ± 15.3% in diastole, and by 29.7 ± 41.3% in systole.

The infarct area was 22.0 ± 3.5% (range: 19.1% to 24%) of the LV area, and had a mean calculated weight of 48.2 ± 6.1 g. Both macro- and microscopically, the posterior papillary muscle was not infarcted. Histology of the infarcted area showed marked thinning of the ventricular wall with no inflammatory response (Fig. 4A and B). Small bundles of cardiomyocytes were present in the subendocardial area (Fig. 4C). The remainder of the wall consisted of bands of fibroblasts alternating with adipocytes within a finely fibrillar background. Ghost cells with a waxy eosinophilic cytoplasm but no residual nuclear material were occasionally observed (Fig. 4D). Small vessels surrounded by occasional normal-looking lymphocytes could be seen near the periphery of the infarct. No foreign body giant cell response was identified. These changes abruptly gave way to a normal appearing myocardium at the periphery of the induced lesion. No epicardial abnormalities were identified.

Table I: Hemodynamic and echocardiographic data before (baseline) and after ethanol injection of OM2-OM3, and at sacrifice.

Parameter	Baseline	After injection	Sacrifice
PAP (mmHg)	25/18	28.6/22	28/13
Cardiac output (l/min)	3.18	2.87	3.92
Aortic pressure (mmHg)	87/66	86/67	72/55
Electrocardiogram	Normal	ST segment elevation	-
Ejection fraction (%)*	56.4 ± 7.0	48.0 ± 9.0	29.6 ± 14.0**,***
LVESD short-axis view (mm)*	31.66 ± 3.4	37.48 ± 3.15	50.6 ± 8.47**
LVEDD short-axis view (mm)*	43.9 ± 3.51	48.82 ± 5.08	58.4 ± 5.94**
Mitral annulus systolic (mm)	29.6 ± 5.6	31.0 ± 2.4	36.25 ± 2.0
Mitral annulus diastolic (mm)	31.54 ± 5.4	33.24 ± 4.7	37.25 ± 2.9
M1-M2 systolic (mm)	21.34 ± 3.36	25.36 ± 2.25	29.6 ± 6.23
M1-M2 diastolic (mm)*	28.16 ± 6.8	32.4 ± 4.64	36.4 ± 5.4**,***
Tethering distance (mm)	37.08 ± 6.0	37.52 ± 6.59	47.2 ± 3.76
Tenting distance (mm)*	4.74 ± 1.35	6.6 ± 1.6	10.25 ± 0.5
Mitral regurgitation*	0	0.2	2.8 ± 0.45**,***
Tricuspid regurgitation*	0.2	0.5	2.1 ± 0.5**,***

Values are mean ± SD.
*Repeated measures analysis of variance (ANOVA) significant, p <0.016; **comparison between baseline and sacrifice, p <0.016; ***comparison between after injection and sacrifice, p <0.016 (all Bonferroni corrected). The differences were not significant for the paired *t*-test between baseline and after injection.
LVEDD: Left ventricular end-diastolic dimension; LVESD: Left ventricular end-systolic dimension; M1: Anteromedial papillary muscle; M2: Posterolateral papillary muscle; PAP: Pulmonary artery pressure.

J Heart Valve Dis
Vol. 14. No. 4
July 2005

Discussion

The incidence of functional IMR after acute myocardial infarction has been reported to be between 13% (14) and 39% (15). Its presence doubles the long-term (five-year) mortality (2), even in cases with mild or moderate regurgitation (16). Although IMR is known to be related to the location and extension of the infarct (17), successful early reperfusion does not reduce mortality (18). Due to the high level of interest in this subject, it is clear that far more questions than answers remain regarding the pathophysiology of IMR and, indeed, of the mechanisms involved in the remodeling of the well-perfused areas that are remote from the infarct (19). In fact, it has been questioned recently whether IMR is the main cause for the poor prognosis of these patients, or simply a reflection of poor LV function secondary to remodeling (20). These questions highlight the need for reproducible chronic experimental models. Furthermore, reduction annuloplasty - which is considered the standard surgical treatment for IMR - has been shown to have a 30% failure rate and no improvement in five-year survival (21). These unsatisfactory results have spurred interest in new surgical alternatives that, initially, must be tested in a large animal model.

Current chronic experimental models have been directed toward inducing either global cardiomyopathy or a localized infarction. Systemic or intracoronary injection of doxorubicin hydrochloride in dogs and goats (22,23), local transmural injection of snake cardiotoxin (24) and coronary microembolization (25,26) result in variable degrees of heart failure, but with absent or unmentioned IMR. The rapid pacing model of cardiomyopathy requires several weeks to create chronic heart failure, but usually achieves only mild or moderate mitral regurgitation that is reversible when pacing is discontinued (27,28). The mechanism responsible for the mitral regurgitation might be different according to the experimental method used. In the rapid pacing ovine model, Timek and associates (29) have described significant mitral annulus dilation (particularly in the septolateral direction) without papillary muscle displacement and leaflet tethering.

In a seminal anatomic study of the coronary artery distribution in sheep, Llaneras et al. (7) demonstrated the absence of collaterals and the very precise and localized effects of selective coronary ligature. Their systematic approach revealed that IMR did not follow the selective ligature of OM1 and OM2, and that occlusion of OM2 and OM3 induced a posterolateral infarct with development of significant IMR at about eight weeks. When ligature of OM4 was added, severe IMR appeared, followed by death within hours. These models, which have been extensively applied by Gorman and associates (4,30), have the disadvantage of needing a thoracotomy to access the selected arteries. Although a thoracotomy is often required to fully instrument the animal when radio-opaque or ultrasound crystals are used, a previous or second thoracotomy is needed either to induce the infarction or to test a particular surgical procedure.

A review of studies on the use of percutaneous alcohol injection into the interventricular septum for the treatment of hypertrophic cardiomyopathy prompted the present authors to consider the possibility of using it to induce IMR by infarcting the myocardium served by OM2 and OM3 (8-10,31).

In the present study, a central IMR appeared in all five surviving sheep between two and four weeks after the procedure, and evolved to 2.8+ at 8 ± 3.1 weeks. These results confirmed the findings of Llaneras et al. (7). In both studies, ligature or EtOH injection of OM2 and OM3 resulted in a localized and well-defined posterolateral infarct and significant IMR. The mitral annulus dilated by 32% in systole and by 13% in diastole, and the interpapillary muscle distance increased by 32% in diastole and by 40% in systole, resulting in an increase in leaflet tethering (+32%) and coaptation (+108%) distances.

The use of TTE allowed each animal to be followed weekly, avoiding a thoracotomy before sacrifice. The TTE findings in the present series confirmed those reported previously in patients (17) and in sheep (5,6). The three-dimensional (3D) data at eight weeks post infarction reported by Otsuji et al. (5) were similar to those of the present two-dimensional (2D) data (Table I). However, while Messas et al. (6) and Otsuji et al. (5) reported significant 3D differences between pre- and immediate post-infarction, the differences obtained with 2D echocardiography did not reach statistical significance (4).

The histology of the EtOH-induced infarct was similar to that described after alcohol septal ablation (32) - that is, an appearance typical of an old, well-defined infarct without signs of inflammation.

Interestingly - and in contrast to the report by Llaneras et al. (7), who noted the presence of an infarcted posterior papillary muscle in all cases - the posterior papillary muscle was found to be intact in all of the present animals, regardless of whether the LV apex was supplied by the left anterior or by the circumflex artery (type A or B heart). The infarct area and degree of IMR were similar in both the Llaneras report (21.4% and 3.18+) and the present model (22% and 2.8+). Despite the difference in papillary muscle status, these similar end results might be explained by the LV remodeling that displaces a perfused posterior papillary muscle. Also, the reports of Messas et al. (6) in sheep and Khankirawatana et al. (33) in humans each

described a paradoxical decrease in IMR severity in the presence of an ischemic papillary muscle.

Recently, in a pig model of alcohol injection into the circumflex arteries, Li et al. (34) showed that the size of the infarct was related to the volume injected, and not to the velocity of delivery (35). In the present study, the maximum volume was arbitrarily limited to 5 ml, and the velocity of injection controlled by hand and in accord with the arrhythmias that occurred during the injection.

Unexpectedly, the development of significant functional tricuspid regurgitation was also noted in all cases. Because of the difficulty imaging the tricuspid valve in sheep, it was not possible to study the mechanism of the ITR and to evaluate RV function. This serendipitous finding, which has not been reported previously in animals subjected to occlusion of the circumflex branches, confirms the similar high incidence found in human cases of IMR (36).

Study limitations

The main limitation of the present study was the small number of animals used. However, the fact that all but one reached the intended objective of inducing significant IMR confirmed the feasibility, simplicity and reproducibility of the method. Additionally, results in sheep cannot be uncritically applied to the human scenario where, for example, diffuse coronary vascular inflammation has been associated with the acute coronary syndromes. Whether the present animal model of IMR following a posterolateral infarct is similar to the clinical situation of an IMR secondary to an inferior infarct remains to be determined (17).

In conclusion, a simple and reproducible percutaneous method to induce significant functional IMR secondary to posterolateral infarct in sheep was developed. Because the technique does not require a thoracotomy to access the targeted vessels, it should reduce morbidity, mortality, pain to the animal, and cost. The procedure allows intact animal studies and, if new surgical procedures are evaluated, avoids the need for second thoracotomy. The present data also show that serial 2D TTE can serve as a reliable method for the evaluation of IMR in sheep. It is hoped that these simple techniques will enhance our understanding of LV remodeling and IMR and, consequently, facilitate the development of new surgical therapies.

Acknowledgements

The authors appreciate the enthusiastic technical assistance of Billi Billington, Leslie Trail and Jessica Vieth in the animal laboratory; Emily Dove for the histology preparations; Tom Maley and Steve Hartigan in the Cardiovascular Catheterization Laboratory; and Jill Roberts for her editorial assistance.

Thomas Joudinaud was supported by a French scholarship from Medtronic France, AMSTER and ADETEC.

References

1. Lamas GA, Mitchell GF, Flaker GC, et al. Clinical significance of mitral regurgitation after acute myocardial infarction. Survival and ventricular enlargement investigators. Circulation 1997;96:827-833
2. Grigioni F, Enriquez-Sarano M, Zehr KJ, Bailey KR, Tajik AJ. Ischemic mitral regurgitation: Long-term outcome and prognostic implications with quantitative Doppler assessment. Circulation 2001;103:1759-1764
3. Hickey MS, Smith LR, Muhlbaier LH, et al. Current prognosis of ischemic mitral regurgitation. Implications for future management. Circulation 1988;78(3 Pt.2):I51-I59
4. Gorman JH, III, Gorman RC, Plappert T, et al. Infarct size and location determine development of mitral regurgitation in the sheep model. J Thorac Cardiovasc Surg 1998;115:615-622
5. Otsuji Y, Handschumacher MD, Liel-Cohen N, et al. Mechanism of ischemic mitral regurgitation with segmental left ventricular dysfunction: Three-dimensional echocardiographic studies in models of acute and chronic progressive regurgitation. J Am Coll Cardiol 2001;37:641-648
6. Messas E, Guerrero JL, Handschumacher MD, et al. Paradoxic decrease in ischemic mitral regurgitation with papillary muscle dysfunction: Insights from three-dimensional and contrast echocardiography with strain rate measurement. Circulation 2001;104:1952-1957
7. Llaneras MR, Nance ML, Streicher JT, et al. Large animal model of ischemic mitral regurgitation. Ann Thorac Surg 1994;57:432-439
8. Lakkis NM, Nagueh SF, Dunn JK, Killip D, Spencer WH, III. Nonsurgical septal reduction therapy for hypertrophic obstructive cardiomyopathy: One-year follow-up. J Am Coll Cardiol 2000;36:852-855
9. Knight C, Kurbaan AS, Seggewiss H, et al. Nonsurgical septal reduction for hypertrophic obstructive cardiomyopathy: Outcome in the first series of patients. Circulation 1997;95:2075-2081
10. Gietzen FH, Leuner CJ, Raute-Kreinsen U, et al. Acute and long-term results after transcoronary ablation of septal hypertrophy (TASH). Catheter interventional treatment for hypertrophic obstructive cardiomyopathy. Eur Heart J 1999;20:1342-1354
11. Helmcke F, Nanda NC, Hsiung MC, et al. Color Doppler assessment of mitral regurgitation with orthogonal planes. Circulation 1987;75:175-183

12. Teichholz LE, Kreulen T, Herman MV, Gorlin R. Problems in echocardiographic volume determinations: Echocardiographic-angiographic correlations in the presence of absence of asynergy. Am J Cardiol 1976;37:7-11
13. Markovitz LJ, Savage EB, Ratcliffe MB, et al. Large animal model of left ventricular aneurysm. Ann Thorac Surg 1989;48:838-845
14. Lehmann KG, Francis CK, Dodge HT. Mitral regurgitation in early myocardial infarction. Incidence, clinical detection, and prognostic implications. TIMI Study Group. Ann Intern Med 1992;117:10-17
15. Barzilai B, Gessler C, Jr., Perez JE, Schaab C, Jaffe AS. Significance of Doppler-detected mitral regurgitation in acute myocardial infarction. Am J Cardiol 1988;61:220-223
16. Hills G, Moller J, Pellikka P, Oh J. Prognostic significance of mitral regurgitation identified using color Doppler echocardiography early after acute myocardial infarction. J Am Coll Cardiol 2004;43(Suppl.A):347
17. Kumanohoso T, Otsuji Y, Yoshifuku S, et al. Mechanism of higher incidence of ischemic mitral regurgitation in patients with inferior myocardial infarction: Quantitative analysis of left ventricular and mitral valve geometry in 103 patients with prior myocardial infarction. J Thorac Cardiovasc Surg 2003;125:135-143
18. Tcheng JE, Jackman JD, Jr., Nelson CL, et al. Outcome of patients sustaining acute ischemic mitral regurgitation during myocardial infarction. Ann Intern Med 1992;117:18-24
19. Abbate A, Bonanno E, Mauriello A, et al. Widespread myocardial inflammation and infarct-related artery patency. Circulation 2004;110:46-50
20. Gorman RC, Gorman JH, III. Does repair of ischemic mitral regurgitation help? Ann Thorac Surg 2003;76:1775-1776; author reply 1776-1777
21. Tahta SA, Oury JH, Maxwell JM, Hiro SP, Duran CMG. Outcome after mitral valve repair for functional ischemic mitral regurgitation. J Heart Valve Dis 2002;11:11-18; discussion 18-19
22. Astra LI, Hammond R, Tarakji K, Stephenson LW. Doxorubicin-induced canine CHF: Advantages and disadvantages. J Card Surg 2003;18:301-306
23. Tessier D, Lajos P, Braunberger E, et al. Induction of chronic cardiac insufficiency by arteriovenous fistula and doxorubicin administration. J Card Surg 2003;18:307-311
24. Rajnoch C, Chachques JC, Berrebi A, Bruneval P, Benoit MO, Carpentier A. Cellular therapy reverses myocardial dysfunction. J Thorac Cardiovasc Surg 2001;121:871-878
25. Sakaguchi G, Sakakibara Y, Tambara K, et al. A pig model of chronic heart failure by intracoronary embolization with gelatin sponge. Ann Thorac Surg 2003;75:1942-1947
26. Suzuki G, Morita H, Mishima T, et al. Effects of long-term monotherapy with eplerenone, a novel aldosterone blocker, on progression of left ventricular dysfunction and remodeling in dogs with heart failure. Circulation 2002;106:2967-2972
27. Byrne MJ, Raman JS, Alferness CA, Esler MD, Kaye DM, Power JM. An ovine model of tachycardia-induced degenerative dilated cardiomyopathy and heart failure with prolonged onset. J Card Fail 2002;8:108-115
28. Timek TA, Dagum P, Lai DT, et al. Tachycardia-induced cardiomyopathy in the ovine heart: Mitral annular dynamic three-dimensional geometry. J Thorac Cardiovasc Surg 2003;125:315-324
29. Timek TA, Dagum P, Lai DT, et al. Pathogenesis of mitral regurgitation in tachycardia-induced cardiomyopathy. Circulation 2001;104(12 Suppl.1):I47-I53
30. Jackson BM, Gorman JH, Moainie SL, et al. Extension of border zone myocardium in postinfarction dilated cardiomyopathy. J Am Coll Cardiol 2002;40:1160-1167; discussion 1168-1171
31. Sigwart U. Non-surgical myocardial reduction for hypertrophic obstructive cardiomyopathy. Lancet 1995;346:211-214
32. Raute-Kreinsen U. Morphology of necrosis and repair after transcoronary ethanol ablation of septal hypertrophy. Pathol Res Pract 2003;199:121-127
33. Khankirawatana B, Khankirawatana S, Mahrous H, Porter TR. Assessment of papillary muscle function using myocardial velocity gradient derived from tissue Doppler echocardiography. Am J Cardiol 2004;94:45-49
34. Li ZQ, Cheng TO, Liu L, et al. Experimental study of relationship between intracoronary alcohol injection and the size of resultant myocardial infarct. Int J Cardiol 2003;91:93-96
35. Cheng TO. In percutaneous transluminal septal myocardial ablation for hypertrophic obstructive cardiomyopathy, it is not the speed of intracoronary alcohol injection but the amount of alcohol injected that determines the resultant infarct size. Circulation 2004;110:e23; author reply e23
36. Koelling TM, Aaronson KD, Cody RJ, Bach DS, Armstrong WF. Prognostic significance of mitral regurgitation and tricuspid regurgitation in patients with left ventricular systolic dysfunction. Am Heart J 2002;144:524-529